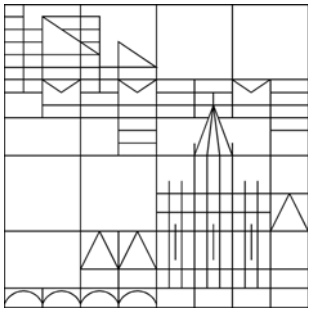

Universität Konstanz

Optimal EPO dosing in hemodialysis patients using a non-linear model predictive control approach

Sabrina Rogg
Doris H. Fuertinger
Stefan Volkwein
Franz Kappel
Peter Kotanko

Konstanzer Schriften in Mathematik

Nr. 372, Januar 2018

ISSN 1430-3558

Konstanzer Online-Publikations-System (KOPS)
URL: http://nbn-resolving.de/urn:nbn:de:bsz:352-2-weqanlx6dq0x5

Journal of Mathematical Biology manuscript No.
(will be inserted by the editor)

Optimal EPO dosing in hemodialysis patients using a non-linear model predictive control approach

S. Rogg · D.H. Fuertinger · S. Volkwein · F. Kappel · P. Kotanko

Received: date / Accepted: date

Abstract Anemia management with erythropoiesis stimulating agents is a difficult task in hemodialysis patients since their response to treatment varies highly. The aim is to stabilize hemoglobin levels within a narrow target window while keeping drug doses low to mitigate side effects and further reduce costs. Based on a model of erythropoiesis, which contains a number of personalized parameters, we present a non-linear model predictive control (NMPC) algorithm for the individualized optimization of epoetin alfa (EPO) doses. The optimal control problem is formulated for a continuous drug administration at a daily or multiple-day constant rate. In each step of the NMPC method the open-loop problem is solved with a projected quasi-Newton method. The controller is successfully tested on various patient data sets and it satisfactorily handles the following challenging problems: bleedings, missed treatments and dosing errors. Moreover, we analyze the effect of restricting EPO administration rates to be constant over a number of weeks.

Keywords optimal control of hyperbolic equations, model predictive control, PDE-constrained optimization, quasi-Newton methods, anemia, erythropoietin

This work has been partially supported by the Renal Research Institute New York, USA.

Sabrina Rogg · Doris H. Fuertinger
Fresenius Medical Care Deutschland GmbH, Bad Homburg, Germany
E-mail: Sabrina.Rogg@fmc-ag.com, Doris.Fuertinger@fmc-ag.com

Stefan Volkwein
Department for Mathematics and Statistics, University of Konstanz, Konstanz, Germany
E-mail: Stefan.Volkwein@uni-konstanz.de

Franz Kappel
Institute for Mathematics and Scientific Computing, University of Graz, Graz, Austria
E-mail: franz.kappel@uni-graz.at

Peter Kotanko
Renal Research Institute New York, New York, USA
E-mail: Peter.Kotanko@rriny.com

Mathematics Subject Classification (2000) 35F45 · 49J24 · 49K20 · 65K10 · 90C30

1 Introduction

According to the 2017 USRDS annual data report, approximately 2.5 million patients were treated world-wide for end-stage renal disease in 2015. In nearly all reporting countries hemodialysis (HD) was the predominant form of dialysis therapy. Around 700 thousand patients were treated in the US, of which 87.7% received HD. Almost all HD patients suffer from chronic anemia due to reduced erythropoietin production in the kidneys. Untreated anemia is associated with poor quality of life and increased morbidity and mortality. Therefore, physicians aim for a partial correction of anemia with erythropoiesis stimulating agents (ESA). In this paper we consider the treatment with epoetin alfa (EPO). Currently, the recommended hemoglobin (Hgb) target range for anemia management is 10 to 12 g/dl (see Mactier et al 2011). Albeit, the KDIGO Work Group recommends not to exceed the limit of 11.5 g/dl in general but suggests to individualize therapy for patients whose quality of life may be improved at Hgb levels above 11.5 g/dl. Usually, dialysis facilities use dosing protocols that work as follows: A starting dose gets specified and based on the resulting Hgb change and wether or not the patient is within the target range the ESA dose gets adjusted. The results of this one size fits all strategy are as follows: The Dialysis Outcomes and Practice Patterns Study (DOPPS) Practice Monitor reports that in the US, since June 2014, the percentage of patients with Hgb above 12 g/dl is 14-15% while 18-20% of patients have a Hgb below 10 g/dl. Moreover, Hgb variability and cycling are well known to occur in HD patients treated with ESA (Berns et al 2003; Fishbane and Berns 2005, 2007). According to Yang et al (2007) a greater Hgb variability is independently associated with higher mortality. The difficulty in treatment is the patients' difference in long-term Hgb response to ESA. The drug concentration in plasma influences the maturation, proliferation and apoptosis of cells in the erythroid lineage. But these cells remain about two weeks unobservable in the bone marrow before released into the bloodstream. Consequently, it is difficult to anticipate the resulting delayed effect of the drug administration. The mathematical model of erythropoiesis presented in Fuertinger et al (2013) predicts patients' erythropoietic response. We utilize this model to design a model-based feedback controller. The successful use of control algorithms for drug dosing has been shown, for example, in Magni et al (2007) and in Bequette (2013). Our model involves a number of patient-specific parameters and parameter estimation is done prior to optimization. Note that insufficient iron availability is not modelled explicitely. A constant availability is assumed and estimated on a per patient level.

The given model equations are coupled hyperbolic partial differential equations (PDEs) where the control variable enters non-linearly. The control strategy we use is called model predictive control (MPC), also known as moving

or receding horizon control. When the underlying model is non-linear, as in our case, the method is referred to as non-linear MPC (NMPC). More details on MPC can be found, e.g., in the books by Grüne and Pannek (2011) and by Rawlings and Mayne (2009). The basic principle of MPC consists in repeatedly solving finite horizon open loop optimal control problems. In each step, an open loop problem is solved. Then, only the first component of the obtained optimal control is applied and the optimization horizon gets pushed. The needed length of the horizon determines the computational effort of the MPC method: the longer the horizon, the slower the numerical solution. Hence, one is searching for the minimal horizon that provides stability of the MPC closed-loop. One reason for the success of MPC in industry is its ability to handle state and control constraints. In our problem, there are only constraints on the EPO administration rate. In 2011, Brier and Gaweda have already published an MPC based algorithm for improved anemia management. But unlike our approach the used predictive model is based on the concept of artificial neural networks (see also Barbieri et al 2016; Brier et al 2010).

This paper is organized as follows: In Section 2 we introduce the control variable and present the model equations. The numerical approximation of these so-called state equations is investigated in Section 3. This involves the formulation of the state equations as abstract Cauchy problems. In Section 4 the optimal control problem is formulated and the NMPC algorithm is described. In Section 5 we present our numerical results of the following experiments: bleedings, missed treatments, wrongly administered doses and the restriction of EPO administration rates to be constant over a number of weeks. We draw some conclusions in Section 6. Finally, all parameters are presented in Appendix A.

2 The model of erythropoiesis

The physiological process under consideration is described by a model of erythropoiesis presented in Fuertinger et al (2013). The different cell types during erythropoiesis are grouped into five population classes: BFU-E, CFU-E, erythroblasts, marrow reticulocytes and erythrocytes (including blood reticulocytes). For each class an age-structured population model is given which describes the development of the respective class subject to a known time-varying EPO concentration in plasma. In the following we first write this concentration as a function of EPO administration rates. Then, we briefly recall the model equations. For the underlying assumptions and more details we refer to Fuertinger (2012), Fuertinger et al (2013).

2.1 The dosing of EPO as the control variable

Let us consider the time interval $[0, T]$ with large final time $T \gg 0$. We assume that EPO can be applied continuously, with a constant administration rate per

day or per multiple days. The EPO rates are given in U/day, where U stands for units. The EPO concentration $E(t)$, $t \in [0,T]$, in plasma is separated into a constant summand $E^{\mathrm{end}} > 0$ modeling the patient's remaining endogenous erythropoietin level and a time-dependent summand $E^{\mathrm{ex}}(t)$ resulting from the administered EPO:

$$E(t) = E^{\mathrm{end}} + E^{\mathrm{ex}}(t) \quad \text{for } t \in [0,T]. \tag{1}$$

For the number $n_u \in \mathbb{N}$ let the days $\{t_u^j\}_{j=1}^{n_u+1}$ with a constant EPO rate in $[t_u^j, t_u^{j+1})$, $j = 1, \ldots, n_u$, be given as

$$0 \le t_u^1 < \ldots < t_u^{n_u+1} \le T. \tag{2}$$

We introduce the associated finite-dimensional control space $\mathcal{U} = \mathbb{R}^{n_u}$. Only non-negative EPO rates with a given upper positive limit $u_{\max} \in \mathbb{R}$ can be applied. Therefore, we are considering the (convex and compact) admissible set

$$\mathcal{U}_{\mathsf{ad}} = \big\{ \boldsymbol{u} = (u_j)_{1 \le j \le n_u} \in \mathcal{U} \,\big|\, 0 \le \boldsymbol{u} \le u_{\max} \big\},$$

where '$\le$' is interpreted componentwise. Throughout, vectors are denoted by boldface letters. Let $\boldsymbol{u} \in \mathcal{U}_{\mathsf{ad}}$ be given. Then, the time- and control-dependent summand $E^{\mathrm{ex}} = E^{\mathrm{ex}}(\cdot\,; \boldsymbol{u})$ satisfies the following initial value problem (cf. Fuertinger et al 2013, equation (12)):

$$\begin{aligned} \frac{\mathrm{d}}{\mathrm{d}t} E^{\mathrm{ex}}(t;\boldsymbol{u}) &= \frac{1}{c_{\mathsf{tbv}}} \left(\sum_{j=1}^{n_u} u_j \chi_j(t) \right) - \lambda E^{\mathrm{ex}}(t;\boldsymbol{u}) \quad \text{for } t \in (0,T], \\ E^{\mathrm{ex}}(0;\boldsymbol{u}) &= E_\circ^{\mathrm{ex}}, \end{aligned} \tag{3}$$

where

$$\chi_j = \chi_{[t_u^j, t_u^{j+1})}, \quad j = 1, \ldots, n_u,$$

are characteristic functions of the intervals $[t_u^j, t_u^{j+1})$, $c_{\mathsf{tbv}} > 0$ stands for the total blood volume, $E_\circ^{\mathrm{ex}}$ is a non-negative initial condition for the exogenous EPO level and $\lambda = \log(2)/T_{1/2} > 0$ is the EPO degradation rate with half-life time $T_{1/2}$. The solution to (3) is given by

$$\begin{aligned} E^{\mathrm{ex}}(t;\boldsymbol{u}) &= e^{-\lambda t} E_\circ^{\mathrm{ex}} + \frac{e^{-\lambda t}}{c_{\mathsf{tbv}}} \sum_{j=1}^{n_u} u_j \int_0^t e^{\lambda s} \chi_j(s)\, \mathrm{d}s \\ &= e^{-\lambda t} E_\circ^{\mathrm{ex}} + \frac{e^{-\lambda t}}{c_{\mathsf{tbv}} \lambda} \left(u_j \big(e^{\lambda t} - e^{\lambda t_u^j} \big) + \sum_{i=1}^{j-1} u_i \big(e^{\lambda t_u^{i+1}} - e^{\lambda t_u^i} \big) \right) \end{aligned} \tag{4}$$

for $t \in [t_u^j, t_u^{j+1})$, $j = 1, \ldots, n_u$. It follows from (4) that $\boldsymbol{u} \mapsto E^{\mathrm{ex}}(\cdot\,; \boldsymbol{u})$ is a function mapping from the admissible set $\mathcal{U}_{\mathsf{ad}} \subset \mathcal{U}$ into $C([0,T])$, where

$C([0,T])$ is the space of all continuous functions from $[0,T]$ to $\mathbb{R}$. Combining (1) and (4) we have

$$E(t;\boldsymbol{u}) = E^{\mathrm{end}} + e^{-\lambda t}E_\circ^{\mathrm{ex}} + \frac{e^{-\lambda t}}{c_{\mathsf{tbv}}\lambda}\left(u_j\big(e^{\lambda t} - e^{\lambda t_u^j}\big) + \sum_{i=1}^{j-1} u_i\big(e^{\lambda t_u^{i+1}} - e^{\lambda t_u^i}\big)\right) \tag{5}$$

for $t \in [t_u^j, t_u^{j+1})$, $j = 1,\dots,n_u$. From (5) and $\lambda > 0$ we infer that

$$E(t;\boldsymbol{u}) \geq E^{\mathrm{end}} + e^{-\lambda T}E_\circ^{\mathrm{ex}} =: E_{\min} > 0 \quad \text{for } t \in [0,T] \text{ and } \boldsymbol{u} \in \mathcal{U}_{\mathsf{ad}}.$$

Thus, we define the interval of possible EPO concentrations

$$\mathcal{E}_{\mathsf{ad}} = [E_{\min}, \infty) = \big\{E \in \mathbb{R} \,\big|\, E \geq E_{\min}\big\}$$

and observe that $E(t;\boldsymbol{u}) \in \mathcal{E}_{\mathsf{ad}}$ holds for all $t \in [0,T]$ and $\boldsymbol{u} \in \mathcal{U}_{\mathsf{ad}}$.

Lemma 1 *The mapping E introduced in* (5)*, has the following properties.*

1) *For every $\boldsymbol{u} \in \mathcal{U}_{\mathsf{ad}}$ the function $E(\cdot\,;\boldsymbol{u}) : [0,T] \to \mathbb{R}$ is continuously differentiable.*
2) *The mapping $E(t;\cdot) : \mathcal{U}_{\mathsf{ad}} \to \mathbb{R}$ is twice continuously differentiable for any $t \in [0,T]$. Its gradient is given as*

$$\nabla_{\boldsymbol{u}} E(t;\boldsymbol{u}) = \frac{e^{-\lambda t}}{c_{\mathsf{tbv}}\lambda}\begin{pmatrix} e^{\lambda t_2} - e^{\lambda t_1} \\ \vdots \\ e^{\lambda t_i} - e^{\lambda t_{i-1}} \\ e^{\lambda t} - e^{\lambda t_i} \\ 0 \\ \vdots \\ 0 \end{pmatrix} \in \mathcal{U}$$

at $t \in [t_u^j, t_u^{j+1})$, $j = 1,\dots,n_u$, and $\boldsymbol{u} \in \mathcal{U}_{\mathsf{ad}}$. Further, the hessian matrix $\nabla_u^2 E(t;\boldsymbol{u}) \in \mathbb{R}^{n_u \times n_u}$ is zero.

Proof The claims follow directly from formula (5). Since $\nabla_{\boldsymbol{u}} E(t;\boldsymbol{u})$ is independent of $\boldsymbol{u}$, the hessian $\nabla_u^2 E(t;\boldsymbol{u})$ is zero. □

2.2 The PDE model of erythropoiesis

For every population class we are given a maturity interval $\Omega_i = (\underline{x}_i, \overline{x}_i) \subset \mathbb{R}$, $1 \leq i \leq 5$, in days. The interval boundaries are given by $\underline{x}_1 = 0$, $\overline{x}_1 = 3 = \underline{x}_2$, $\overline{x}_2 = 8 = \underline{x}_3$, $\overline{x}_3 = 13 = \underline{x}_4$, $\overline{x}_4 = 15.5$, $\underline{x}_5 = 0$, whereas the red blood cell (RBC) lifespan $\overline{x}_5$ is patient-dependent. Ma et al (2017) have measured this shortened (compared to healthy individuals) RBC lifespan in HD patients to be in the range of 37.7 to 115.8 days. Throughout, x denotes the maturity of a respective cell. We have a flux of cells from each population class to

the subsequent one. For example, when a CFU-E cell has reached maximum age it leaves the class and becomes an erythroblast with minimum maturity. Furthermore, stem cells commit to the erythroid lineage at a constant rate $S_0 > 0$. Suppose that for given $\boldsymbol{u} \in \mathcal{U}_{\mathsf{ad}}$ and $E_\circ^{\mathrm{ex}} \geq 0$ the EPO concentration $E = E(t;\boldsymbol{u})$ is given as (5). We follow Fuertinger et al (2013) and write all five state equations in the form

$$\begin{aligned} y_t(t,x) &= \kappa(x;E(t;\boldsymbol{u}))y(t,x) - v(E(t;\boldsymbol{u}))y_x(t,x) && \text{in } Q,\\ y(t,\underline{x}) &= g(t;E(t;\boldsymbol{u})) && \text{in } (0,T],\\ y(0,x) &= y_0(x) && \text{in } \Omega, \end{aligned} \tag{6}$$

with the spatial domain $\Omega = (\underline{x},\overline{x}) \subset \mathbb{R}$, the time-space cylinder $Q = (0,T)\times\Omega$ and the initial condition y_0. The solution $y(t,x)$ to (6) denotes the cell density of the respective cell population with maturity x at time t. The function v describes the maturation velocity and $\kappa(\cdot)$ is of form $\beta - \alpha(\cdot)$, where $\beta > 0$ describes the profileration rate and α the rate of apoptosis. Actually, the occurring sigmoid functions depend on the bounded (patient-dependent) parameter vector $\boldsymbol{\mu} = (\mu_i) \in \mathbb{R}_+^{10}$ with $\mathbb{R}_+ = \{s \in \mathbb{R} \,|\, s > 0\}$. We refer to Section A, where all fixed and all individualized parameters, which we utilize in our numerical experiments, are listed. To simplify the notation we do not indicate dependencies on $\boldsymbol{\mu}$. The functions for the different classes read as follows:

$$\begin{aligned} v(E) &= \begin{cases} \nu(E) & \text{if } i = 4,\\ 1 & \text{otherwise,} \end{cases} \qquad \kappa(x;E) = \begin{cases} \beta_1 & \text{if } i = 1,\\ \beta_2 - \alpha_2(E) & \text{if } i = 2,\\ \beta_3 & \text{if } i = 3,\\ -\alpha_4 & \text{if } i = 4,\\ -\alpha_5(x;E) & \text{if } i = 5, \end{cases}\\ y_0(x) &= y_{0i}(x) \text{ for } i = 1,\dots,5, \quad g(t;E) = \begin{cases} S_0 & \text{if } i = 1,\\ y_1(t,\overline{x}_1) & \text{if } i = 2,\\ y_2(t,\overline{x}_2) & \text{if } i = 3,\\ y_3(t,\overline{x}_3)/\nu(E) & \text{if } i = 4,\\ \nu(E)\, y_4(t,\overline{x}_4) & \text{if } i = 5, \end{cases} \end{aligned} \tag{7}$$

where the real-valued functions α_2 and ν are given by

$$\alpha_2(E) = \frac{\mu_1}{1+e^{\mu_2 E-\mu_3}}, \quad \nu(E) = \frac{\mu_4-\mu_5}{1+e^{-\mu_6 E+\mu_7}} + \mu_5, \tag{8}$$

for $E \in \mathcal{E}_{\mathsf{ad}}$ and the function

$$\alpha_5 : \Omega_5 \times \mathcal{E}_{\mathsf{ad}} \to \mathbb{R},$$

$$\alpha_5(x;E) = \alpha_5^0 + \begin{cases} \min\left(\dfrac{\mu_8}{E^{\mu_9}}, \mu_{10}\right) & \text{if } x \in \widehat{\Omega}_5,\ E \in \mathcal{E}_{\mathsf{ad}} \text{ with } E \leq \tau_E,\\ 0 & \text{otherwise,} \end{cases}$$

stands for the erythrocytes mortality rate with an EPO threshold $\tau_E > 0$ for neocytolysis. The (closed) non-empty interval $\widehat{\Omega}_5 \subsetneq \Omega_5$ denotes the age interval, where neocytolysis is possible.

Lemma 2 *The mappings $\alpha_2, \nu : \mathcal{E}_{\mathsf{ad}} \to \mathbb{R}$ are continuously differentiable.*

Proof The claim follows directly from (8). □

We denote the five state equations by (**S.1**)-(**S.5**) and the coupled system by (**S**).

2.3 Total RBC population

If the erythrocytes population density is known, the *total RBC population* $P = P(t)$, $t \in [0, T]$, is given as

$$P[\boldsymbol{y}](t) = \int_{\Omega_5} y_5(t, x)\,\mathrm{d}x \quad \text{for } t \in [0, T], \tag{9}$$

where $\boldsymbol{y} = (y_i)_{1 \le i \le 5}$ solve the state system (**S**).

2.4 Regularization of the equation for the erythrocytes

In Section 4 we will introduce a non-linear optimal control problem which we solve numerically by utilizing first-order necessary optimality conditions. For that reason we have to differentiate the state system (**S**) with respect to the state variable $\boldsymbol{y} = (y_i)_{1 \le i \le 5}$ and the control variable $\boldsymbol{u} = (u_j)_{1 \le j \le n_u}$. From Lemma 1 we know that $\boldsymbol{u} \mapsto E(t; \boldsymbol{u})$ is continuously differentiable for every $t \in [0, T]$. Moreover, α_2 and ν are continuously differentiable by Lemma 2. However, the mapping $\mathcal{E}_{\mathsf{ad}} \ni E \mapsto \alpha_5(x; E)$ is non-differentiable for every $x \in \widehat{\Omega}_5$. Therefore, we have to regularize α_5 in order to get smooth state equations.

First we rewrite the mapping α_5. For that reason we introduce the Heaviside function $H : \mathbb{R} \to \mathbb{R}$ defined as

$$H(s) = 0 \text{ for } s \le 0 \quad \text{and} \quad H(s) = 1 \text{ for } s > 0.$$

Then, the mortality rate can equivalently be written as

$$\alpha_5(x; E) = \alpha_5^0 + \chi_{\widehat{\Omega}_5}(x) H(\tau_E - E) R(E), \quad \text{for } x \in \Omega_5 \text{ and } E \in \mathcal{E}_{\mathsf{ad}} \tag{10}$$

with

$$R(E) = \min\left(\frac{\mu_8}{E^{\mu_9}}, \mu_{10}\right) \quad \text{for } E \in \mathcal{E}_{\mathsf{ad}}. \tag{11}$$

For $\varepsilon > 0$ we utilize the following regularized Heaviside function $H^\varepsilon : \mathbb{R} \to \mathbb{R}$

$$H^\varepsilon(s) = \begin{cases} 0 & \text{if } s \leq 0, \\ \frac{s^4}{\varepsilon^6}\left(10s^2 - 24\varepsilon s + 15\varepsilon^2\right) & \text{for } s \in (0, \varepsilon), \\ 1 & \text{if } s \geq \varepsilon. \end{cases}$$

Notice that the function

$$F^\varepsilon(s, \tau) = (s - \tau)H^\varepsilon(\tau - s) + \tau, \quad s, \tau \in \mathbb{R}$$

is an approximation of $\min(s, \tau)$. Thus, the function R defined in (11) can be regularized as

$$R^\varepsilon(E) = F^\varepsilon\left(\frac{\mu_8}{E^{\mu_9}}, \mu_{10}\right) \quad \text{for } E \in \mathcal{E}_{\mathsf{ad}}$$

which allows us to replace the non-smooth coefficient function α_5 by the smooth (with respect to E) mapping

$$\alpha_5^\varepsilon(x; E) = \alpha_5^0 + \chi_{\widehat{\Omega}_5}(x)H^\varepsilon(\tau_E - E)R^\varepsilon(E) \quad \text{for } x \in \Omega_5 \text{ and } E \in \mathcal{E}_{\mathsf{ad}}. \quad (12)$$

Lemma 3 *For every $x \in \Omega_5$ the mapping $\alpha_5^\varepsilon(x; \cdot) : \mathcal{E}_{\mathsf{ad}} \to \mathbb{R}$ is continuously differentiable.*

Proof The claim follows directly from (12) because of $E_{\min} > 0$. □

In the sequel we replace α_5 in (7) by α_5^ε and hence κ by κ^ε to account for the regularized fifth state equation which we denote by $(\mathbf{S}.\mathbf{5}^\varepsilon)$. Let $(\mathbf{S}^\varepsilon)$ be the state system $(\mathbf{S.1})$-$(\mathbf{S.4})$ and $(\mathbf{S}.\mathbf{5}^\varepsilon)$.

3 Numerical approximation of the state equations

3.1 Discretization of the state equations

For the numerical solution of the age-structured population models we first compare a discretization based on semigroup theory and Legendre polynomials (see Fuertinger et al 2013) with a discretization carried out by finite differences utilizing an upwind scheme (cf. Strikwerda 2004).

3.1.1 Discretization using semigroup theory and Legendre polynomials

In this subsection we first formulate the five state equations as abstract Cauchy problems. Then, these are approximated by semigroups acting on finite dimensional subspaces spanned by shifted Legendre polynomials.

The state equations as abstract Cauchy problems: Let us also refer the reader to, e.g., Ito and Kappel (2002) and Kappel and Zhang (1993) for results on evolution operators and their approximation.

Lemma 4 *Let $\varepsilon > 0$ and $E(\cdot\,;\boldsymbol{u})$ be given by (5) for an arbitrarily chosen $\boldsymbol{u} \in \mathcal{U}_{\mathsf{ad}}$. Then, the mappings $t \mapsto v(E(t;\boldsymbol{u}))$ and $t \mapsto \kappa^{\varepsilon}(x;E(t;\boldsymbol{u}))$ are continuously differentiable on $[0,T]$ for every $x \in \Omega$.*

Proof The claim follows from Lemmas 1-3 using $E_{\min} > 0$. □

Now, for $n \in \mathbb{N}$ we introduce the function

$$\delta_n(x) = \begin{cases} -2n^2\left(x - \underline{x} - \dfrac{1}{n}\right) & \text{for } \underline{x} \le x \le \underline{x} + \dfrac{1}{n}, \\ 0 & \text{for } \underline{x} + \dfrac{1}{n} < x \le \overline{x}. \end{cases}$$

Note that $\{\delta_n\}_{n\in\mathbb{N}}$ is a sequence of functions approximating the δ-distribution. Let y_n, $n \in \mathbb{N}$, be a mild solution of the non-homogeneous Cauchy problem

$$\frac{\mathrm{d}}{\mathrm{d}t}\, y_n(t) = \mathcal{A}^{\varepsilon}(E(t;\boldsymbol{u}))y_n(t) + g(t;E(t;\boldsymbol{u}))\delta_n \text{ for } t \in (0,T], \quad y_n(0) = y_0 \quad (13)$$

for given $\boldsymbol{u} \in \mathcal{U}_{\mathsf{ad}}$, where the linear operator $\mathcal{A}^{\varepsilon}(E)$, $E \in \mathcal{E}_{\mathsf{ad}}$, is defined as

$$\begin{aligned} \operatorname{dom}\mathcal{A}^{\varepsilon}(E) = \big\{ & \varphi \in L^2(\Omega) \,\big|\, \varphi \text{ is absolutely continuous on } \overline{\Omega}, \\ & \varphi(\underline{x}) = 0, v(E)\varphi' - \kappa^{\varepsilon}(\cdot\,;E)\varphi \in L^2(\Omega)\big\}, \\ \mathcal{A}^{\varepsilon}(E)\varphi = {} & -v(E)\varphi' + \kappa^{\varepsilon}(\cdot\,;E)\varphi \text{ for } \varphi \in \operatorname{dom}\mathcal{A}^{\varepsilon}(E). \end{aligned}$$

Let us assume that $\lim_{n\to\infty} y_n(t) = y(t)$ in $L^2(\Omega)$ holds for $t \in [0,T]$, where y is the solution to (6).

Since the range for the attribute is different for the cell populations considered, it is useful to normalize these attributes such that the range of the normalized attribute ξ is $[0,1]$. In order to achieve this we set $w = \overline{x} - \underline{x} > 0$ and define the mapping

$$h : [0,1] \to \overline{\Omega} = [\underline{x}, \overline{x}], \quad h(\xi) = \underline{x} + w\xi \quad \text{for } \xi \in [0,1]$$

with its inverse given by

$$h^{-1} : \overline{\Omega} \to [0,1], \quad h^{-1}(x) = \frac{x - \underline{x}}{w} \quad \text{for } x \in \overline{\Omega}.$$

We denote by $L^2_w(0,1)$ the Hilbert space $L^2(0,1)$ endowed with the weighted inner product

$$\langle \tilde{\varphi}, \tilde{\phi} \rangle_w = w \int_0^1 \tilde{\varphi}(\xi)\tilde{\phi}(\xi)\,\mathrm{d}\xi = w \langle \tilde{\varphi}, \tilde{\phi} \rangle_{L^2(0,1)} \quad \text{for } \tilde{\varphi}, \tilde{\phi} \in L^2_w(0,1).$$

The induced norm is $\|\cdot\|_w = w^{1/2}\|\cdot\|_{L^2(0,1)}$. The Hilbert spaces $L^2_\omega(0,1)$ and $L^2(\Omega)$ are isomorphic with the isomorphism $\Xi : L^2(\Omega) \to L^2_w(0,1)$ and its inverse $\Xi^{-1} : L^2_w(0,1) \to L^2(\Omega)$ given by

$$\Xi\varphi = \varphi \circ h \text{ for } \varphi \in L^2(\Omega), \quad \Xi^{-1}\tilde{\varphi} = \tilde{\varphi} \circ h^{-1} \text{ for } \tilde{\varphi} \in L^2_w(0,1).$$

We set

$$\tilde{\delta}_n(\xi) = (\Xi\delta_n)(\xi) = \begin{cases} -2n^2\left(w\xi - \dfrac{1}{n}\right) & \text{for } 0 \le w\xi \le \dfrac{1}{n}, \\ 0 & \text{for } \dfrac{1}{n} < w\xi \le 1. \end{cases}$$

Then, instead of (13), we consider the normalized Cauchy problem in $L^2_w(0,1)$:

$$\frac{\mathrm{d}}{\mathrm{d}t}\,\tilde{y}_n(t) = \tilde{\mathcal{A}}^\varepsilon(E(t;\boldsymbol{u}))y_n(t) + g(t;E(t;\boldsymbol{u}))\tilde{\delta}_n \text{ for } t \in (0,T],\ \tilde{y}_n(0) = \tilde{y}_0, \quad (14)$$

where the operator $\tilde{\mathcal{A}}^\varepsilon(E)$, $E \in \mathcal{E}_{\mathsf{ad}}$, is defined as

$$\begin{aligned} \operatorname{dom}\tilde{\mathcal{A}}^\varepsilon(E) = \big\{\tilde{\varphi} \in L^2_w(0,1) \,\big|\, &\tilde{\varphi} \text{ is absolutely continuous on } [0,1], \\ &\tilde{\varphi}(0) = 0, v(E)\tilde{\varphi}' - \kappa^\varepsilon(h(\cdot);E)\tilde{\varphi} \in L^2_w(0,1)\big\}, \\ \tilde{\mathcal{A}}^\varepsilon(E)\tilde{\varphi} = -v(E)\tilde{\varphi}' + \kappa^\varepsilon(h(\cdot);E)\tilde{\varphi} &\text{ for } \tilde{\varphi} \in \operatorname{dom}\tilde{\mathcal{A}}^\varepsilon(E) \end{aligned}$$

and $\tilde{y}_0 = y_0 \circ h : [0,1] \to \mathbb{R}$ holds.

Approximation: We introduce a discretization of the Cauchy problem (14); cf. Kappel and Zhang (1993), and Fuertinger et al (2013). Let us define the functions

$$e_j(\xi) = \frac{1}{\sqrt{w}}\,L_j(-1+2\xi), \quad 0 \le \xi \le 1, \quad j \in \mathbb{N}_0 = \{0\} \cup \mathbb{N},$$

where L_j denotes the j-th Legendre polynomial. The sequence $\{e_j\}_{j\in\mathbb{N}_0}$ is an orthogonal sequence in $L^2_w(0,1)$ with

$$\langle e_j, e_k\rangle_w = 0 \text{ for } j \ne k \quad \text{and} \quad \|e_j\|^2_w = \langle e_j, e_j\rangle_w = \frac{1}{2j+1}. \quad (15)$$

For $N \in \mathbb{N}_0$ we introduce the N-dimensional subspace $X_N \subset L^2_w(0,1)$ by

$$X_N = \operatorname{span}\big\{e_0, \dots, e_{N-1}\big\}.$$

Let $\mathcal{P}_N : L^2_w(0,1) \to X_N$ be the orthogonal projection defined as

$$\mathcal{P}_N\tilde{\varphi} = \sum_{j=0}^{N-1} \frac{\langle\tilde{\varphi}, e_j\rangle_w}{\|e_j\|^2_w}\,e_j \quad \text{for } \tilde{\varphi} \in L^2_w(0,1).$$

The approximating delta distribution $\tilde{\delta}_N$ on X_N is defined by

$$\langle\tilde{\delta}_N, \tilde{\varphi}\rangle_w = \tilde{\varphi}(0) \quad \text{for } \tilde{\varphi} \in X_N. \quad (16)$$

For any $E \in \mathcal{E}_{\mathsf{ad}}$ we define the approximating linear operator $A_N^\varepsilon(E) : X_N \to X_N$ by

$$\tilde{A}_N^\varepsilon(E)\varphi = -\frac{v(E)}{w}\,\varphi' + \mathcal{P}_N\big(\kappa^\varepsilon(h(\cdot);E)\varphi\big) - \tilde{\delta}_N\varphi(0) \quad \text{for } \varphi \in X_N.$$

Note that the projection $\mathcal{P}_N$ needs only be applied onto $\kappa^\varepsilon\big(h(\cdot);E\big)\varphi$ in case of the erythrocytes model equation due to $\varphi' \in X_N$ for $\varphi \in X_N$. Now, the discretization of (14) is given as

$$\begin{aligned} \frac{\mathrm{d}}{\mathrm{d}t}\,\tilde{y}_N(t) &= \tilde{A}_N^\varepsilon(E(t;\boldsymbol{u}))\tilde{y}_N(t) + g(t;E(t;\boldsymbol{u}))\tilde{\delta}_N \quad \text{for } t \in (0,T], \\ \tilde{y}_N(0) &= \mathcal{P}_N\tilde{y}_0. \end{aligned} \tag{17}$$

If $\tilde{y}_N$ is a solution to (17), the function

$$y_N(t,\cdot) = \Xi^{-1}\big(\tilde{y}_N(t,\cdot)\big) = \tilde{y}_N(t,h^{-1}(\cdot)) : \Omega \to \mathbb{R}, \quad t \in [0,T],$$

is an approximate solution to (13). Using (15), (16) and

$$\tilde{y}_N(t,\xi) = \sum_{j=0}^{N-1} \tilde{\mathrm{y}}_j(t)e_j(\xi), \quad (t,\xi) \in [0,T]\times[0,1],$$

we derive the Galerkin scheme

$$\begin{aligned} \|e_i\|_w^2\,\frac{\mathrm{d}}{\mathrm{d}t}\,\tilde{\mathrm{y}}_i(t) &= \sum_{j=0}^{N-1} \tilde{\mathrm{y}}_j(t)\langle A_N^\varepsilon(E(t;\boldsymbol{u}))e_j, e_i\rangle_w + g(t;E(t;\boldsymbol{u}))e_i(0), \\ \tilde{\mathrm{y}}_i(0) &= \frac{\langle \tilde{y}_0, e_i\rangle_w}{\|e_i\|_w^2} \end{aligned} \tag{18}$$

for $i = 0,\dots,N-1$. Setting

$$\begin{aligned} \tilde{\boldsymbol{y}}(t) &= \big(\tilde{\mathrm{y}}_{i-1}(t)\big)_{1\le i\le N} && \text{for } t \in [0,T], \\ \boldsymbol{A}^\varepsilon(E) &= \left(\frac{\langle A_N^\varepsilon(E)e_{j-1}, e_{i-1}\rangle_w}{\|e_{i-1}\|_w^2}\right)_{1\le i,j\le N} && \text{for } E \in \mathcal{E}_{\mathsf{ad}}, \\ \boldsymbol{d} &= \left(\frac{e_{i-1}(0)}{\|e_{i-1}\|_w^2}\right)_{1\le i\le N}, \quad \tilde{\boldsymbol{y}}_0 = \left(\frac{\langle \tilde{y}_0, e_{i-1}\rangle_w}{\|e_{i-1}\|_w^2}\right)_{1\le i\le N} \end{aligned}$$

we can express (18) as the following system of N ordinary differential equations

$$\frac{\mathrm{d}}{\mathrm{d}t}\,\tilde{\boldsymbol{y}}(t) = \boldsymbol{A}^\varepsilon(E(t;\boldsymbol{u}))\tilde{\boldsymbol{y}}(t) + g(t;E(t;\boldsymbol{u}))\boldsymbol{d} \text{ for } t \in (0,T], \quad \tilde{\boldsymbol{y}}(0) = \tilde{\boldsymbol{y}}_0. \tag{19}$$

Theorem 1 *Let $E(\cdot\,;\boldsymbol{u})$ given by (5) for an arbitrarily chosen $\boldsymbol{u} \in \mathcal{U}_{\mathsf{ad}}$. Moreover, $g(\cdot\,;E) : [0,T] \to \mathbb{R}$ is assumed to be piecewise continuous for every $E \in \mathcal{E}_{\mathsf{ad}}$. Then, the function*

$$\tilde{\boldsymbol{y}}(t) = e^{\int_0^t \boldsymbol{A}^\varepsilon(E(s;\boldsymbol{u}))\,\mathrm{d}s}\tilde{\boldsymbol{y}}_0 + \left(\int_0^t e^{\int_\tau^t \boldsymbol{A}^\varepsilon(E(s;\boldsymbol{u}))\,\mathrm{d}s} g(\tau;E(\tau;\boldsymbol{u}))\,\mathrm{d}\tau\right)\boldsymbol{d} \tag{20}$$

is the only one that satisfies (19) at every time instance, where $g(\cdot\,;E)$ is continuous for every $E \in \mathcal{E}_{\mathsf{ad}}$. Furthermore, $\tilde{\boldsymbol{y}} \in H^1(0,T;\mathbb{R}^N)$ holds.

Proof 1) We first show that (20) satisfies (19). Due to Lemma 4 the mapping $\boldsymbol{A}^\varepsilon(E(\cdot\,;\boldsymbol{u})) : [0,T] \to \mathbb{R}^{N\times N}$ is continuously differentiable for every $\boldsymbol{u} \in \mathcal{U}_{\mathsf{ad}}$. We obtain for any $t \in (0,T]$, where $g(\cdot\,;E)$ is continuous

$$\begin{aligned}\frac{\mathrm{d}}{\mathrm{d}t}\tilde{\boldsymbol{y}}(t) &= \boldsymbol{A}^\varepsilon(E(t;\boldsymbol{u}))e^{\int_0^t \boldsymbol{A}^\varepsilon(E(s;\boldsymbol{u}))\,\mathrm{d}s}\tilde{\boldsymbol{y}}_\circ + g(\tau;E(t;\boldsymbol{u}))\boldsymbol{d}\\ &\quad + \boldsymbol{A}^\varepsilon(E(t;\boldsymbol{u}))\bigg(\int_0^t e^{\int_\tau^t \boldsymbol{A}^\varepsilon(E(s;\boldsymbol{u}))\,\mathrm{d}s} g(\tau;E(\tau;\boldsymbol{u}))\,\mathrm{d}\tau\bigg)\boldsymbol{d}\\ &= \boldsymbol{A}^\varepsilon(E(t;\boldsymbol{u}))\tilde{\boldsymbol{y}}(t) + g(t;E(t;\boldsymbol{u}))\boldsymbol{d}.\end{aligned}$$

Further, if we choose $t = 0$ in (20) we get $\tilde{\boldsymbol{y}}(0) = \tilde{\boldsymbol{y}}_0$. Hence, $\tilde{\boldsymbol{y}}$ satisfies (19) at every time instance, where $g(\cdot\,;E)$ is continuous.

2) Uniqueness: Assume there exist two solutions $\tilde{\boldsymbol{y}}^1$, $\tilde{\boldsymbol{y}}^2$ to (19). We set $\tilde{\boldsymbol{z}} = \tilde{\boldsymbol{y}}^1 - \tilde{\boldsymbol{y}}^2$. Then, it follows that

$$\frac{\mathrm{d}}{\mathrm{d}t}\,\tilde{\boldsymbol{z}}(t) = \boldsymbol{A}^\varepsilon(E(t;\boldsymbol{u}))\tilde{\boldsymbol{z}}(t)$$

for all $t \in (0,T]$, where $g(\cdot\,;E)$ is continuous. Since $\boldsymbol{A}^\varepsilon(E(\cdot\,;\boldsymbol{u}))$ and $\tilde{\boldsymbol{z}}$ are continuous, we can extend the derivative of $\tilde{\boldsymbol{z}}$ by $\boldsymbol{A}^\varepsilon(E(t;\boldsymbol{u}))\tilde{\boldsymbol{z}}(t)$ for all $t \in (0,T]$. Furthermore, we have $\tilde{\boldsymbol{y}}^1(0) = \tilde{\boldsymbol{y}}^2(0)$. From Gronwall's inequality we infer that $\tilde{\boldsymbol{z}}(0) = 0$ in $[0,T]$, which implies $\tilde{\boldsymbol{y}}^1 = \tilde{\boldsymbol{y}}^2$ in $[0,T]$. □

Remark 1 1) Due to Theorem 1 the solution

$$\tilde{y}_N(t,\xi) = \sum_{j=0}^{N-1} \tilde{\mathrm{y}}_j(t)e_j(\xi), \quad (t,\xi) \in [0,T]\times[0,1],$$

to (17) belongs to $H^1(0,T;L^2_w(0,1))$ provided $g(\cdot\,;E) : [0,T] \to \mathbb{R}$ is piecewise continuous for every $E \in \mathcal{E}_{\mathsf{ad}}$.

2) To solve (19) a time integration method has to be applied. In our numerical experiments we apply the implicit Euler method. ◊

3.1.2 Discretization by central upwind differences

For comparison we consider a (standard) finite difference scheme for (6). We introduce an equidistant spatial and temporal grid by

$$\begin{aligned} x^i &= \underline{x} + i\Delta x \quad \text{for } i = 0,\dots,N_x, \quad \Delta x = \frac{\overline{x}-\underline{x}}{N_x},\\ t^j &= j\Delta t \qquad\quad \text{for } j = 0,\dots,N_t, \quad \Delta t = \frac{T}{N_t}.\end{aligned}$$

We denote by y^{ji} the approximation of the state y at $(t^j,x^i) \in \overline{Q}$. For given $\boldsymbol{u} \in \mathcal{U}_{\mathsf{ad}}$, $E^{\mathrm{ex}}_\circ \geq 0$ let $E = E(\cdot\,;\boldsymbol{u})$ be given by (5). Recall that $v(E(t;\boldsymbol{u})) = 1$ holds for $i = 1,2,3,5$. In this case the Courant-Friedrichs-Levy (CFL) condition (cf. Strikwerda 2004, Section 1.6) yields $\Delta t \leq \Delta x$ so that we choose $\Delta t = \Delta x$

for $i = 1, 2, 3, 5$. For $i = 4$ we have $v(E(t; \boldsymbol{u})) = \nu(E(t; \boldsymbol{u}))$. Then, the more general CFL condition reads

$$|\nu(E(t; \boldsymbol{u}))| \Delta t \leq \gamma \Delta x, \quad \text{for all } t \in [0, T] \tag{21}$$

with a constant $\gamma \in (0, 1)$. Since $|\nu(E(t; \boldsymbol{u}))| < 2$ holds on $[0, T]$ and $\mathcal{U}_{\mathsf{ad}}$, we choose $\Delta t = \Delta x/2$ for $i = 4$ in order to ensure (21). Summarizing, we set

$$\Delta t = \begin{cases} \dfrac{\Delta x}{2} & \text{if } i = 4, \\ \Delta x & \text{if } i = 1, 2, 3, 5, \end{cases} \quad \text{and} \quad \eta = \frac{\Delta t}{\Delta x} = \begin{cases} \dfrac{1}{2} & \text{if } i = 4, \\ 1 & \text{if } i = 1, 2, 3, 5. \end{cases} \tag{22}$$

Disregarding the source term g in (6) central upwind differences read (see, e.g., Quarteroni 2009, p. 348; Trangenstein 2009, pp. 12 and 98)

$$y^{j+1,i} = \begin{cases} y^{ji} - \eta\big(y^{ji} - y^{j,i-1}\big) + \dfrac{\beta_1}{2}\big(y^{ji} + y^{j,i-1}\big), & i = 1, \\ y^{ji} - \eta\big(y^{ji} - y^{j,i-1}\big) \\ \qquad + \dfrac{\beta_2 - \alpha_2(E(t^j; \boldsymbol{u}))}{2}\big(y^{ji} + y^{j,i-1}\big), & i = 2, \\ y^{ji} - \eta\big(y^{ji} - y^{j,i-1}\big) + \dfrac{\beta_3}{2}\big(y^{ji} + y^{j,i-1}\big), & i = 3, \\ y^{ji} - \eta\nu(E(t^j; \boldsymbol{u}))\big(y^{ji} - y^{j,i-1}\big) - \dfrac{\alpha_4}{2}\big(y^{ji} + y^{j,i-1}\big), & i = 4, \\ y^{ji} - \eta\big(y^{ji} - y^{j,i-1}\big) - \alpha_5^{\varepsilon}(x; E(t^j; \boldsymbol{u}))y^{j,i-1}, & i = 5 \end{cases} \tag{23}$$

with

$$y^{0,i} = y_0(x_i) \text{ for } i = 0, \ldots, N_x, \quad y^{j,0} = g(t^j; E(t^j; \boldsymbol{u})) \text{ for } j = 0, \ldots, N_t.$$

For $i = 2$ the source term is added using an upwinding discretization and for $i = 1, 3, 4, 5$ we apply a backwards in space approximation. For more details we refer to Bermudez and Vazquez (1994). Note that we discard from viewing the discrete values as approximations to cell averages (see LeVeque 1992, p. 97f).

3.2 Comparison of the two discretization schemes

We solve the state equations consecutively for a given control $\boldsymbol{u} \in \mathcal{U}_{\mathsf{ad}}$ using the discretization by Legendre polynomials and by upwind differences. The corresponding approximate total RBC populations (cf. (9)) at the discrete time points $t^j = j\Delta t$, $j = 0, \ldots, N_t$, with $\Delta t = 0.01$, are denoted by P_L^j and P_U^j, respectively. Notice that the total RBC population is actually the quantity of interest and not the underlying two-dimensional density. For the discretization based on Legendre polynomials we take $N = 15$ together with the time step size $\Delta t = 0.01$ for all five equations. The finite difference solution requires the smaller step size $\Delta t/2$ for the first four equations to obtain a reliable approximation of the exact population. Here, the spatial step size Δx

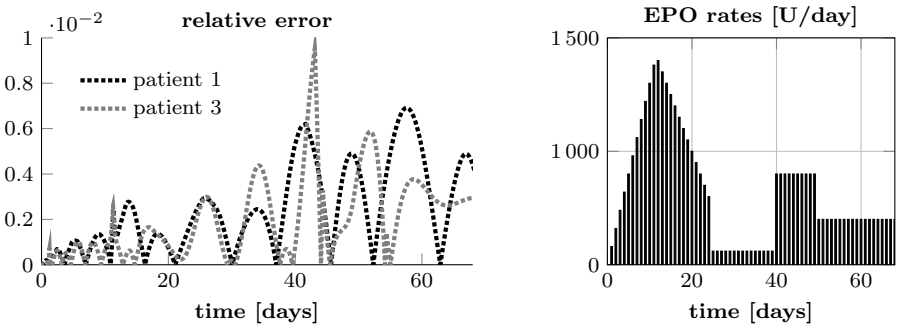

Fig. 1 Relative deviation $|P_L^j - P_U^j|/|P_U^j|$, $j = 0, \dots, N_t$, where P_L^j and P_U^j denote the approximate total RBC populations computed using Legendre polynomials and by upwind differences, respectively, at the discrete time points $t^j = j\Delta t$ with $\Delta t = 0.01$, for the fixed control shown in the right plot.

is chosen according to (22). We measure the accuracy of the Legendre based population by means of the relative deviations $|P_L^j - P_U^j|/|P_U^j|$, $j = 0, \dots, N_t$. For patients 1 and 3 these deviations are shown in Figure 1 together with the applied EPO rates. As can be seen, the relative deviations are below 10^{-2}. The underlying central upwind solutions are built on very fine grids whereas the discretization with Legendre polynomials leads to a uniform spatial dimension of only $N = 15$. Therefore, we can compute the latter one in average three times faster.

Motivated by our numerical experiments we utilize the discretization based on Legendre polynomials for the optimal EPO dosing. Let $\boldsymbol{u} \in \mathcal{U}_{\mathsf{ad}}$ be a given control variable and $E(\cdot\,;\boldsymbol{u})$ be given by (5). Then, the five state variables $(y_i)_{1\le i\le 5}$ solving $(\mathbf{S}^\varepsilon)$ are approximated by the functions

$$y_{i,N}(t,\cdot) = \tilde{y}_{i,N}(t, h^{-1}(\cdot)) = \sum_{j=0}^{N} \tilde{\mathrm{y}}_{ij}(t) e_j(h^{-1}(\cdot)) \in L^2(\Omega) \tag{24a}$$

for $i = 1, \dots, 5$, where the coefficient vector $\tilde{\boldsymbol{y}}_i = (\tilde{\mathrm{y}}_{i,j-1})_{1\le j\le N}$ satisfies (19) for the choice $i \in \{1, \dots, 5\}$ written as

$$\begin{aligned} &\frac{\mathrm{d}}{\mathrm{d}t}\,\tilde{\boldsymbol{y}}_i(t) = \boldsymbol{A}_i^\varepsilon(E(t;\boldsymbol{u}))\tilde{\boldsymbol{y}}_i(t) + g_i(t;E(t;\boldsymbol{u}))\boldsymbol{d}_i \quad \text{for } t \in (0,T], \\ &\tilde{\boldsymbol{y}}_i(0) = \tilde{\boldsymbol{y}}_{0i}. \end{aligned} \tag{24b}$$

Due to Theorem 1 we define the non-linear solution operator

$$\mathcal{S}_N : \mathcal{U}_{\mathsf{ad}} \to \bigtimes_{i=1}^{5} H^1(0,T;\mathbb{R}^N),$$

where $\tilde{\boldsymbol{y}} = (\tilde{\boldsymbol{y}}_i)_{1\le i\le 5} = \mathcal{S}_N(\boldsymbol{u})$ satisfies (24). Then, the discretized total RBC population is given by (cf. (9))

$$P_N[\tilde{\boldsymbol{y}}](t) = \sum_{j=0}^{N} \tilde{\mathrm{y}}_{5,j}(t) \int_{\Omega_5} e_j(h^{-1}(x))\,\mathrm{d}x = \tilde{\mathrm{y}}_{5,0}(t)\,\omega_5^{1/2} \quad \text{for } t \in [0,T] \tag{25}$$

where again $\tilde{\boldsymbol{y}} = (\tilde{\boldsymbol{y}}_i)_{1\le i\le 5}$ satisfies (24).

4 The optimal EPO dosing

In this section we formulate the optimal EPO dosing as an optimal control problem on the long time horizon $[0, T]$.

4.1 The optimal control problem

The aim is to stabilize a patient's Hgb level within a target window. Equivalently, we formulate the optimal control problem for the patient's number of RBCs with a target range of $0 < \underline{P}^d$ to $\overline{P}^d$ cells. In order to achieve our goal, we measure and penalize the deviation of the total RBC population from a desired population P^d with $\underline{P}^d \le P^d \le \overline{P}^d$ over the whole time horizon $[0, T]$:

$$\hat{J}_N(\boldsymbol{u}) = \frac{1}{2}\sum_{j=1}^{n_u} \gamma_j \left|u_j\right|^2 + \frac{\sigma_\Omega}{2}\int_0^T \left|P_N[\tilde{\boldsymbol{y}}](t) - P^d\right|^2 \mathrm{d}t, \tag{26}$$

where the discretized total RBC population $P_N[\tilde{\boldsymbol{y}}]$ has been introduced in (25) and $\tilde{\boldsymbol{y}} = \mathcal{S}_N(\boldsymbol{u})$ satisfies (24). Further, $\gamma_1, \dots, \gamma_{n_u} > 0$ are regularization parameters and σ_Ω is a non-negative weight. Now, the optimal control problem is formulated as follows:

$$\min \hat{J}_N(\boldsymbol{u}) \quad \text{subject to} \quad \boldsymbol{u} \in \mathcal{U}_{\mathsf{ad}}. \tag{$\hat{\mathbf{P}}$}$$

Remark 2 Note that ($\hat{\mathbf{P}}$) is a non-linear optimization problem. Hence, ($\hat{\mathbf{P}}$) is non-convex, so that several local minima might exist. ◊

4.2 The NMPC method

Since the patient data can change over time, ($\hat{\mathbf{P}}$) can not be treated as an open-loop problem. Rather, we are interested to derive a state feedback law

$$E(t; \boldsymbol{u}) = \boldsymbol{\Phi}(t; \tilde{\boldsymbol{y}}(t)) \quad \text{for } t \in [0, T]. \tag{27}$$

Thus, if the mapping $\boldsymbol{\Phi}$ is known, we know the optimal EPO concentration $E(\cdot\,; \boldsymbol{u})$ at time t provided the state vectors $\tilde{\boldsymbol{y}} = (\tilde{\boldsymbol{y}}_i)_{1\le i\le 5}$ can be (partially) estimated or measured. In this case the optimal state trajectories are given by the closed loop system

$$\begin{aligned} &\frac{\mathrm{d}}{\mathrm{d}t}\,\tilde{\boldsymbol{y}}_i(t) = \boldsymbol{A}_i^{\varepsilon}\big(\boldsymbol{\Phi}(t; \tilde{\boldsymbol{y}}(t))\big)\tilde{\boldsymbol{y}}_i(t) + g_i\big(t; \boldsymbol{\Phi}(t; \tilde{\boldsymbol{y}}(t))\big)\boldsymbol{d}_i \quad \text{for } t \in (0, T], \\ &\tilde{\boldsymbol{y}}_i(0) = \tilde{\boldsymbol{y}}_{0i} \end{aligned} \tag{28}$$

for $i = 1, \ldots, 5$. It is well-known that the mapping $\boldsymbol{\Phi}$ is given by the solution to an unsteady Hamilton-Jacobi-Bellman equation, which is a non-linear hyperbolic equation of first-order with the spatial dimension N. For $N > 10$ this problem can not be solved numerically so that other techniques have to be applied. Here, we apply an NMPC approach to get a state feedback of the form (27), where a state feedback law is computed by solving a sequence of smaller time horizon problems. Let all time intervals of constant administration rates be of same length $\Delta_t > 0$ and

$$T = L\Delta_t \quad \text{for } L \in \mathbb{N}.$$

Suppose we are at time $t_\circ \in [0, T - M\Delta_t]$ and consider the time horizon $[t_\circ, t_\mathsf{f}]$ with $t_\mathsf{f} = t_\circ + M\Delta_t$, $M \in \mathbb{N}$ and $M\Delta_t \ll T$. Next we introduce a notation for the days

$$\{t_u^{j_l}\}_{l=1}^{n(t_\circ)+1} \subset \{t_u^1, \ldots, t_u^{n_u+1}\} \subset [0, T] \quad \text{with} \quad t_\circ \le t_u^{j_1} < \ldots < t_u^{j_{n_u(t_\circ)+1}} \le t_\mathsf{f},$$

which belong to the current horizon $[t_\circ, t_\mathsf{f}]$; cf. (2). At $t_\circ$ we are given the initial conditions $\tilde{\boldsymbol{y}}_\circ = (\tilde{\boldsymbol{y}}_{\circ i})_{1 \le i \le 5}$ and $E^{\mathrm{ex}}(t_\circ) = E_\circ^{\mathrm{ex}}$. Then, we define the cost functional on the time horizon $[t_\circ, t_\mathsf{f}] \subset [0, T]$ with $0 \le t_\circ < t_\mathsf{f}$ and $t_\mathsf{f} - t_\circ \ll T$:

$$\begin{aligned} \hat{J}_N(\boldsymbol{u}; t_\circ, \tilde{\boldsymbol{y}}_\circ, E_\circ^{\mathrm{ex}}) = \frac{1}{2} \sum_{l=1}^{n_u(t_\circ)} \gamma_{j_l} |u_{j_l}|^2 + \frac{\sigma_\Omega}{2} \int_{t_\circ}^{t_\mathsf{f}} \left| P_N[\tilde{\boldsymbol{y}}](t) - P^d \right|^2 \mathrm{d}t \\ + \frac{\sigma_\mathsf{f}}{2} \left| P_N[\tilde{\boldsymbol{y}}](t_\mathsf{f}) - P^d \right|^2, \end{aligned} \tag{29}$$

where the coefficient vector $\tilde{\boldsymbol{y}}_i = (\tilde{\mathrm{y}}_{i,j-1})_{1 \le j \le N}$ satisfies

$$\begin{aligned} &\frac{\mathrm{d}}{\mathrm{d}t} \tilde{\boldsymbol{y}}_i(t) = \boldsymbol{A}_i^\varepsilon(E(t; \boldsymbol{u})) \tilde{\boldsymbol{y}}_i(t) + g_i(t; E(t; \boldsymbol{u})) \boldsymbol{d}_i \quad \text{for } t \in (t_\circ, t_\mathsf{f}], \\ &\tilde{\boldsymbol{y}}_i(t_\circ) = \tilde{\boldsymbol{y}}_{\circ i} \end{aligned} \tag{30}$$

for $i = 1, \ldots, 5$. In (29) we add a summand penalizing the deviation of the population at the final time t_f. For $\mathcal{U}(t_\circ) = \mathbb{R}^{n_u(t_\circ)}$ we define the admissible set

$$\mathcal{U}_{\mathsf{ad}}(t_\circ) = \left\{ \boldsymbol{u} \in \mathcal{U}(t_\circ) \,\middle|\, 0 \le \boldsymbol{u} \le u_{\mathsf{max}} \right\}.$$

Now, the controller predicts the future evolution of the system under control over the prediction horizon $M\Delta_t$, the cost functional $\hat{J}_N(\boldsymbol{u}; t_\circ, \tilde{\boldsymbol{y}}_\circ, E_\circ^{\mathrm{ex}})$ gets minimized and we obtain an optimal control vector for the given time period. Then, (only) the first component of the optimal control vector is applied and yields new initial conditions for the next initial time point $t_\circ + \Delta_t$, to where the finite horizon gets pushed. This strategy allows us to react to parameter perturbations which, e.g., are caused by missed treatments, dosing errors or bleedings in our application. In Algorithm 1 we summarize the NMPC method. The iterative computation of the control $\boldsymbol{u}$ can be seen in line 5 where in each iteration the first component of the optimal open loop solution

Algorithm 1 (NMPC algorithm)

Require: Initial state $\tilde{\boldsymbol{y}}_\circ = (\tilde{\boldsymbol{y}}_{\circ i})_{1\le i\le 5}$, initial exogenous EPO level $E^{\mathrm{ex}}_\circ$ at time $t_\circ = 0$;
1: Set $\boldsymbol{u} = []$;
2: **for** $\ell = 1, 2, \dots, L$ **do**
3: Set $t_\circ = (\ell-1)\Delta_t$ and $t_{\mathsf{f}} = t_\circ + M\Delta_t$;
4: Compute a (numerical) solution $\bar{\boldsymbol{u}}^{(\ell)} = (\bar{u}_{j_l}^{(\ell)})_{1\le l\le n_u(t_\circ)}$ to

$$\min \hat{J}_N(\boldsymbol{u}; t_\circ, \tilde{\boldsymbol{y}}_\circ, E^{\mathrm{ex}}_\circ) \quad \text{s.t.} \quad \boldsymbol{u} \in \mathcal{U}_{\mathsf{ad}}(t_\circ); \tag{$\hat{\mathbf{P}}(t_\circ)$}$$

5: Set $\boldsymbol{u} = [\boldsymbol{u}, \bar{u}_1^{(\ell)}]$ and define the NMPC feedback value

$$\boldsymbol{\Phi}^M(t; \tilde{\boldsymbol{y}}_\circ) = E(t; \bar{\boldsymbol{u}}_1^{(\ell)}) \quad \text{for } t \in [t_\circ, t_\circ + \Delta_t];$$

6: Compute the associated state

$$\begin{aligned} &\frac{\mathrm{d}}{\mathrm{d}t}\tilde{\boldsymbol{y}}_i(t) = \boldsymbol{A}_i^\varepsilon(E(t;\boldsymbol{u}))\tilde{\boldsymbol{y}}_i(t) + g_i(t; E(t;\boldsymbol{u}))\boldsymbol{d}_i \quad \text{for } t \in (t_\circ, t_\circ + \Delta_t], \\ &\tilde{\boldsymbol{y}}_i(t_\circ) = \tilde{\boldsymbol{y}}_{\circ i} \end{aligned}$$

for $1 \le i \le 5$;
7: Set $\tilde{\boldsymbol{y}}_\circ = \tilde{\boldsymbol{y}}(t_\circ + \Delta_t)$ and $E^{\mathrm{ex}}_\circ = E(t_\circ + \Delta_t, \boldsymbol{u})$;
8: **end for**

to problem $(\hat{\mathbf{P}}(t_\circ))$ from line 4 is appended to the already given control vector. Then, this control is applied on the corresponding time interval $[t_\circ, t_\circ + \Delta_t]$ and the initial condition for the next iteration is set to $\tilde{\boldsymbol{y}}(t_\circ + \Delta_t)$; see line 7. If the state vectors can be measured or estimated based on measurements, the new initial condition $\tilde{\boldsymbol{y}}_\circ$ in line 7 can be set therewith.

4.3 Numerical solution of the open-loop problem $(\hat{\mathbf{P}}(t_\circ))$

It remains to discuss how the open-loop problem in line 4 of Algorithm 1 is numerically solved. In this work we apply a projected BFGS method with Armijo linesearch as described in Kelley (1999, Section 5.5.3). This requires to compute the gradient $\nabla \hat{J}_N = (\partial_{u_{j_l}} \hat{J}_N)_{1\le l\le n_u(t_\circ)}$ at $\boldsymbol{u} = (u_{j_l})_{1\le l\le n_u(t_\circ)} \in \mathcal{U}_{\mathsf{ad}}(t_\circ)$. It is given by

$$\begin{aligned} &\partial_{u_{j_l}} \hat{J}_N(\boldsymbol{u}; t_\circ, \tilde{\boldsymbol{y}}_\circ, E^{\mathrm{ex}}_\circ) = \gamma_{j_l} u_{j_l} \\ &+ \sum_{i=1}^{5} \int_{t_\circ}^{t_{\mathsf{f}}} \left(\frac{\partial E}{\partial u_{j_l}}(t;\boldsymbol{u}) \Big(\frac{\partial \boldsymbol{A}_i^\varepsilon}{\partial u_{j_l}}(E(t;\boldsymbol{u}))\tilde{\boldsymbol{y}}_i(t) - \frac{\partial g_i}{\partial u_{j_l}}(E(t;\boldsymbol{u}))\boldsymbol{d}_i \Big) \right)^\top \boldsymbol{D}_\omega \tilde{\boldsymbol{p}}_i(t)\,\mathrm{d}t, \end{aligned}$$

with the adjoint variable $\tilde{\boldsymbol{p}} = (\tilde{\boldsymbol{p}}_i)_{1\le i\le 5}$, where $\tilde{\boldsymbol{p}}_i$ satisfies

$$\begin{aligned} -\frac{\mathrm{d}}{\mathrm{d}t}\tilde{\boldsymbol{p}}_i(t) &= \boldsymbol{D}_\omega^{-1} \boldsymbol{A}_i^\varepsilon(E(t;\boldsymbol{u}))^\top \boldsymbol{D}_\omega \tilde{\boldsymbol{p}}_i(t) \\ &\quad + \boldsymbol{D}^{-1}\boldsymbol{D}_i \boldsymbol{D} q_i(t; E(t;\boldsymbol{u})) \quad \text{for } t \in (t_\circ, t_{\mathsf{f}}], \\ \tilde{\boldsymbol{p}}_i(t_{\mathsf{f}}) &= 0, \end{aligned} \tag{31}$$

for $i = 1, \dots, 5$, with $\boldsymbol{D}_\omega = \mathrm{diag}(\frac{1}{2j+1} \mid j = 0, \dots, N)$, $\boldsymbol{D}_i = \mathrm{diag}(\boldsymbol{d}_i)$, $i = 1, \dots, 5$ and

$$q_i(t; E) = \begin{cases} \omega_{i+1}^{-1/2} \tilde{\boldsymbol{p}}_{i+1}(t) & \text{if } i = 1, 2, \\ \omega_4^{-1/2} \tilde{\boldsymbol{p}}_4(t) / \nu(E) & \text{if } i = 3, \\ \omega_5^{-1/2} \nu(E) \tilde{\boldsymbol{p}}_5(t) & \text{if } i = 4. \end{cases}$$

5 Numerical results

For our numerical experiments we have chosen the data sets from five patients which capture the main occurring characteristics. These parameters can be looked up in Table 8. The constant endogenous erythropoietin concentration E^{end} for example is once far above the threshold for neocytolysis ($\tau_E = 80$), twice just slightly below and twice clearly smaller. The aim was to find a general optimization setting that works for diverse data sets. Note that the desired amount of RBCs depends on the patients' total blood volume and hence differs. But the values correspond to the single Hgb target window of 10-12 g/dl. The desired Hgb level is set to 10.5 g/dl. We choose this lower value because in case of an overshoot the Hgb can not be pulled down actively but one has to wait till it decreases of itself. For computation of the population densities we scale the hyperbolic equations by 10^8 which is legitimate since the equations are linear with respect to the state variables y_i, $i = 1, \dots, 5$. For discretization we use $N = 15$ Legendre polynomials and the time step size $\Delta t = 0.01$.

5.1 Uncontrolled erythrocytes population

We begin by taking a look at the patients' predicted total RBC population without EPO treatment. As can be seen exemplarily in Figure 2 the total population is running in a steady state far below the target range. This state of anemia would be critical for the patients since it increases cardiovascular disease and death risk (Strippoli et al, 2004). In the following we show how the NMPC algorithm is able to correct anemia in the patients' models.

5.2 NMPC

5.2.1 Settings

Throughout we consider a total time period of 24 weeks, i.e. $T = 168$ days. Excluding our last experiment, the days $\{t_u^j\}_{j=1}^{n_u+1}$ are given by $\{0, 1, \dots, 168\}$ and the length of the NMPC horizon is four weeks. Hence, we set $\Delta_t = 1$, $M = 28$ and $L = 168$. There are cases where a smaller horizon can as well lead to satisfactory results but four weeks has worked without exception. The fact

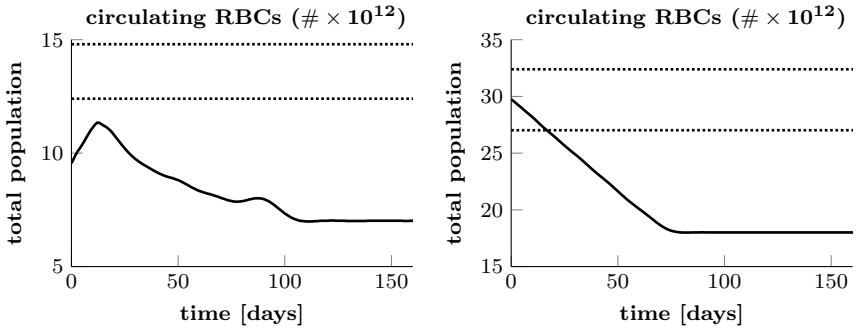

(a) Patient 1 (b) Patient 2

Fig. 2 Uncontrolled erythrocytes populations. The dotted lines mark the target range.

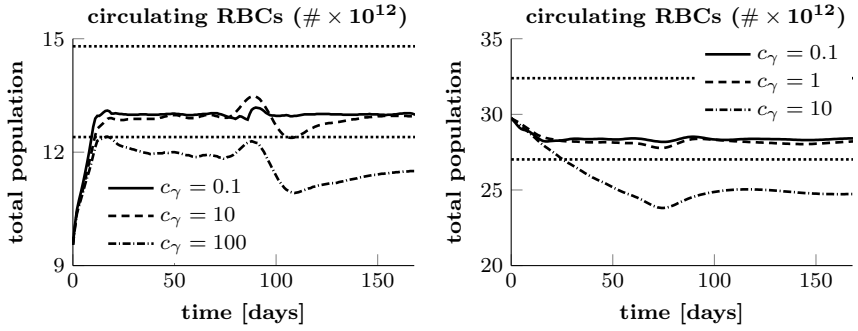

(a) Patient 1 (b) Patient 2

Fig. 3 Optimal RBC population for different values c_γ for patients 1 and 2. The dotted lines mark the target range.

that the cells remain about two weeks in the bone marrow (first four classes) before released into the bloodstream explains the need for this length. The maximum EPO rate is set to $u_{\max} = 1000$ U/day. Given the time horizon $M\Delta_t$ we set

$$\sigma_\Omega = \frac{10^4}{M\Delta_t\big(\overline{P}^d - \underline{P}^d\big)^2}, \quad \sigma_{\mathsf{f}} = \frac{10^3}{\big(\overline{P}^d - \underline{P}^d\big)^2}, \quad \gamma_j \equiv \frac{c_\gamma}{M\Delta t}, \tag{32}$$

where only the parameter c_γ is chosen in an individualized manner.

We start by testing the NMPC algorithm for different constants c_γ. This parameter penalizes control costs in the objective functional. A larger c_γ results in a stronger penalization of control costs, i.e. the optimizer must try to bring and keep the total RBC population in the target range with less EPO. In Figure 3 we present the results for patients 1 and 2. For both patients the value $c_\gamma = 0.1$ is the right choice for control costs penalization in the sense that it allows to accurately control the population around the target state P^d. Having a look at the corresponding EPO rates in Figures 4 and 5 one can see

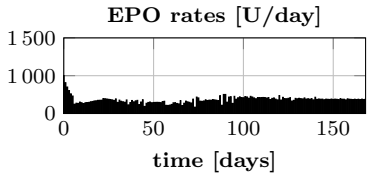

(a) $c_\gamma = 100$

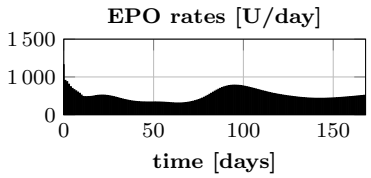

(b) $c_\gamma = 10$

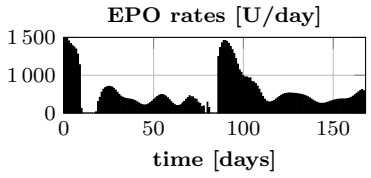

(c) $c_\gamma = 0.1$

Fig. 4 Patient 1: optimal EPO rates for different values c_γ.

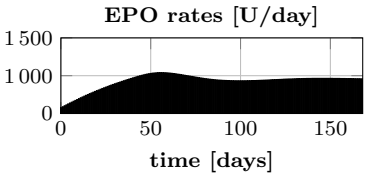

(a) $c_\gamma = 10$

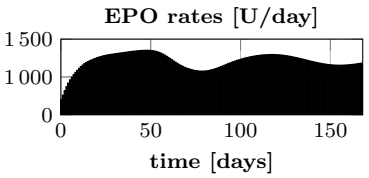

(b) $c_\gamma = 1$

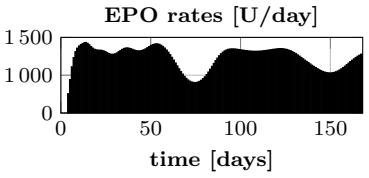

(c) $c_\gamma = 0.1$

Fig. 5 Patient 2: optimal EPO rates for different values c_γ.

Table 1 Total EPO doses for different values c_γ for patients 1 and 2.

	Patient 1			Patient 2		
c_γ	0.1	10	100	0.1	1	10
total dose [U]	48 323	42 683	30 616	121 354	119 114	71 706

that patient 2 requires a lot higher doses. It is actually about 2.5 times as much; see Table 1. For $c_\gamma = 10$ the results for patient 1 are still quite good while this penalization is obviously too high for patient 2. Still, for $c_\gamma = 1$ the total population for patient 2 remains as well nicely within the target range. Using $c_\gamma = 100$ for patient 1 is then also too strong.

Our focus lies more on the RBC population than the total amount of administered EPO. Thus, we choose c_γ such that the penalization of control costs does not block the NMPC algorithm from nicely controlling the erythrocytes population. The above test we have also done for the other patients. For patient 5 the value $c_\gamma = 0.1$ is fine as well while patients 3 and 4 require a weaker penalization of $c_\gamma = 0.01$. Concluding, with $c_\gamma = 0.01$ the total RBC population of all patients can be greatly controlled only that for patients 1,2 and 5

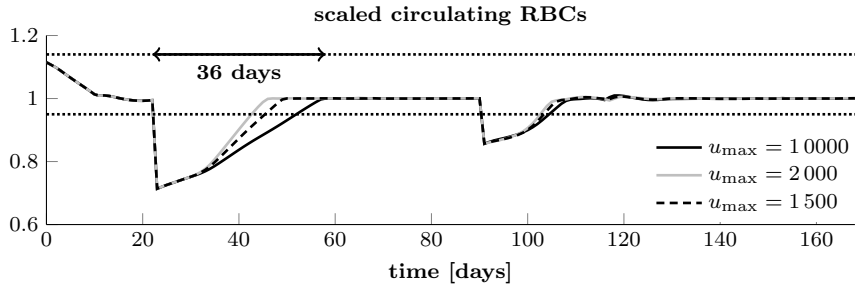

(a) Patient 4: bleeding at day 22 (29% of P^d lost) and at day 80 (14% of P^d lost)

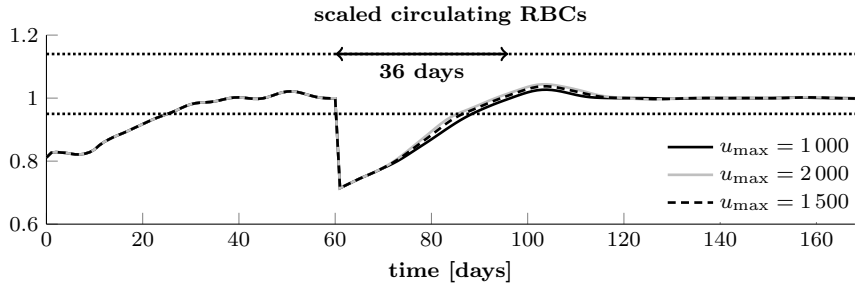

(b) Patient 3: bleeding at day 60 (29% of P^d lost)

Fig. 6 Bleeding patients 3 and 4: total RBC population scaled by P^d for different values $u_{\max}$ after the first bleeding. Up to the first bleeding $u_{\max}$ equals 1 000. The dotted lines mark the target range.

an equally good result can as well be obtained with $c_\gamma = 0.1$ and consequently lower EPO doses.

5.2.2 Bleeding

In the following we analyze how the NMPC algorithm handles a sudden and unforeseen bleeding. Notice that this is a frequent complication in HD patients. For a better comparability between different patients we plot the total RBC population scaled by P^d. This is done in Figure 6 for patients 3 and 4 for a bleeding which corresponds to a loss of around 29% of P^d. Patient 4 has a fast recovery time so that we add a later smaller bleeding of 14% of P^d. According to Pottgiesser et al (2008) the mean recovery time period after a blood donation of 550 ml is 36 days (range 20-59). This average recovery time is added as a vertical arrow to Figure 6. We run the optimization such that we first keep the maximum EPO rate at 1 000 U/day and after the first bleeding we increase $u_{\max}$ to 1 500 U/day or to 2 000 U/day to see if a higher maximum rate results in a considerable smaller recovery time. We observe that the NMPC algorithm is reacting to the bleeding by directly administering the maximum available EPO dose over a certain period of time. The EPO rates are shown in Figures 7 and 8. For a higher $u_{\max}$ this higher amount is administered but

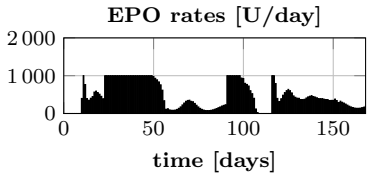

(a) $u_{\max} = 1\,000$

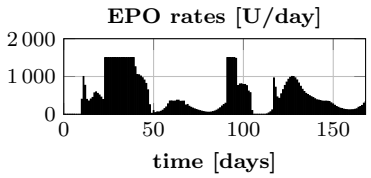

(b) $u_{\max} = 1\,500$

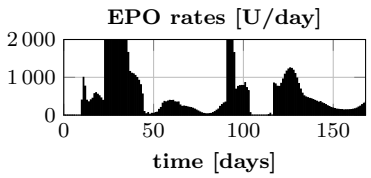

(c) $u_{\max} = 2\,000$

Fig. 7 Bleeding patient 4: EPO rates for different values $u_{\max}$ after the first bleeding. Up to the first bleeding $u_{\max}$ equals 1 000. The first bleeding is at day 22 (29% of P^d lost) and the second at day 80 (14% of P^d lost).

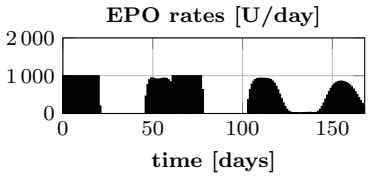

(a) $u_{\max} = 1\,000$

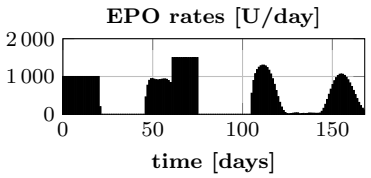

(b) $u_{\max} = 1\,500$

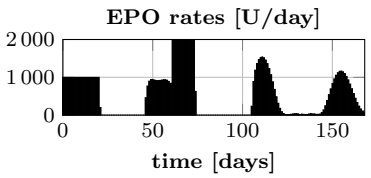

(c) $u_{\max} = 2\,000$

Fig. 8 Bleeding patient 3: EPO rates for different values $u_{\max}$ after the bleeding. Up to the bleeding $u_{\max}$ equals 1 000. The bleeding is at day 60 (29% of P^d lost).

for a shorter period of time. Hence, the total drug amount, see Table 2, is at most 16% and 13% higher for the largest maximum rate. The recovery time after the first bleeding for patient 4 can be significantly reduced from about 36 to about 25 days by allowing higher administration rates. For patient 3 the differences are minor. The reason is parameter μ_2. Its value for patient 3 is 0.008 while it equals 0.011 for patient 4. This parameter determines the slope of the sigmoid function

$$\alpha_2(E) = \frac{\mu_1}{1 + e^{\mu_2 E - \mu_3}} \quad \text{for } E \in \mathcal{E}_{\mathsf{ad}} = \left\{ E \in \mathbb{R} \,\middle|\, E \geq E_{\min} \right\}$$

(cf. (8)) which describes apoptosis of CFU-E cells. A larger μ_2 results in a faster decrease of α_2 with increasing EPO concentration, i.e. less cells die with increasing EPO concentration. The two sigmoid functions are presented in Figure 13.

Table 2 Bleeding patients 3 and 4: total EPO doses for different values $u_{\max}$ after the first bleeding. Up to the first bleeding $u_{\max}$ equals 1 000. For patient 3 the first bleeding is at day 22 (29% of P^d lost) and the second at day 80 (14% of P^d lost). In case of patient 3 there is only one bleeding at day 60 (29% of P^d lost).

	Patient 4			Patient 3		
$u_{\max}$	1 000	1 500	2 000	1 000	1 500	2 000
total dose [U]	79 124	86 148	91 853	83 980	90 109	94 948

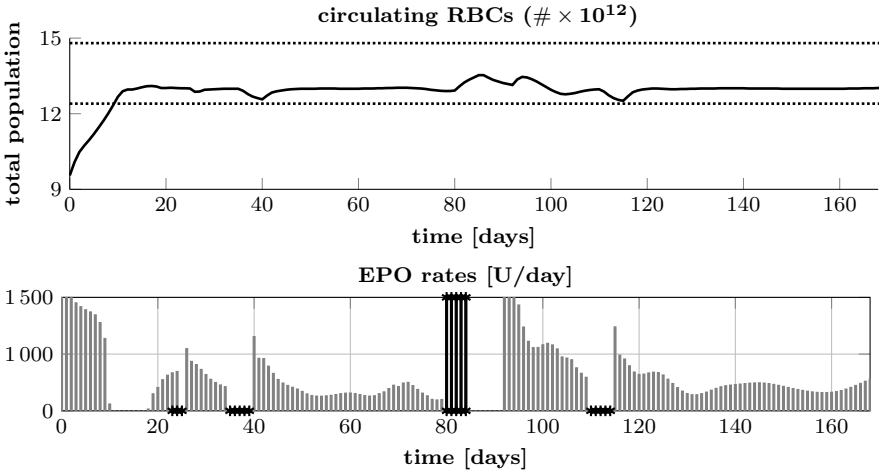

Fig. 9 Patient 1: optimal EPO rates and RBC population for missed treatments on days 23-25, 35-39, 110-114 and on days 80-84 the maximum EPO rate is administered by mistake.

5.2.3 Missed treatments/dosing errors

In this section we simulate that patients have obtained wrong EPO rates or have missed treatments (not known in advance). In Figure 9 we present the results for patient 1 with missed treatments on days 23-25, 35-39 and 110-114. In addition, on days 80-84 the maximum amount $u_{\max} = 1\,000$ gets administered by mistake. Missing a treatment leads to a certain direct drop in the total RBC population. After every period of missed treatments the algorithm compensates for these by applying a higher EPO rate which is then gradually reduced in order to smoothly reincrease the erythrocytes population. After the period when the maximum amount is wrongly applied the algorithm administers nothing so that the RBC population decreases and that an overshoot is avoided. But interestingly, it then restarts with the maximum amount before dropping on the desired level and a minor reincrease is even accepted. In doing so it achieves to balance the delayed effect of having administered no drug before and a later drastic drop-down is avoided. The total administered EPO dose is 50 853 U/day.

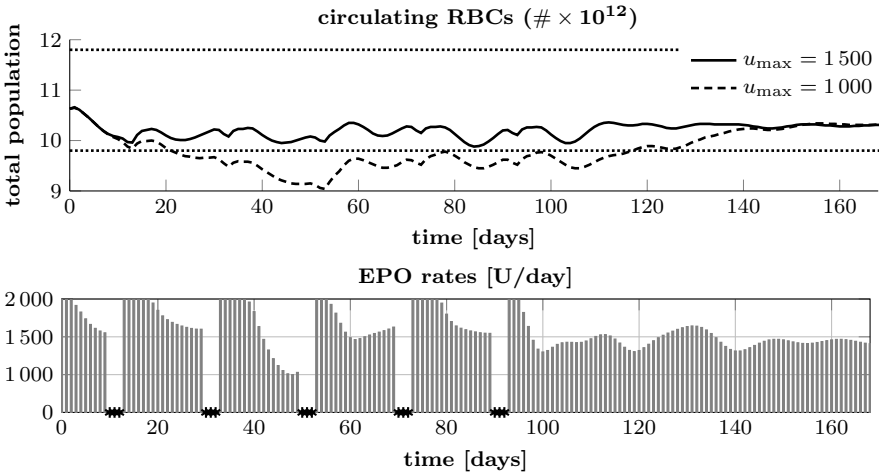

Fig. 10 Patient 5: optimal EPO rates and RBC population for missed treatments on days 10-12, 30-32, 50-52, 70-72, 90-92 and $u_{\max} = 1\,500$. In addition, the optimal RBC population for $u_{\max} = 1\,000$ is shown in the upper plot.

In Figure 10 we present the results for periodically missed EPO administrations. More precisely, starting at day ten, every two weeks three days drop out. This scheme is chosen for analyzing if a periodic missing of treatments results in periodic administration rates. But as can be seen, the EPO rates after each period of missed treatments look different and the NMPC alogithm achieves to keep the RBC population within the desired range if $u_{\max}$ is set to 1 500 U/day. Patient 5 demands high EPO rates so that the RBC population falls below the target range if $u_{\max}$ equals 1000 U/day. Note that the erythrocytes population can be kept within the target range for $u_{\max} = 1\,000$ if there are no missed treatments. The total administered EPO doses belonging to Figure 10 are 167 848 U/day ($u_{\max} = 1\,500$) and 150 921 U/day ($u_{\max} = 1\,000$).

5.2.4 Constant EPO rates

Finally, we investigate the effect of enlarging the period of constant EPO rates from 1 day ($\Delta_t = 1$) to 1 week ($\Delta_t = 7$), 2 weeks ($\Delta_t = 14$), 3 weeks ($\Delta_t = 21$) and 4 weeks ($\Delta_t = 28$). The length of the NMPC horizon is set to 4 weeks (constant period 1 week), 6 weeks (constant period 2 or 3 weeks) and 8 weeks (constant period 4 weeks). In order to penalize control costs likewise for the different constant periods the parameter c_γ in equation (32) gets multiplied by the number of days in the respective constant period.

The results for patient 4 are exemplarily shown in Figures 11 and 12. The visible range in Figure 11 is exactly the lower half of the target window for patient 4. The erythrocytes populations for the different constant periods stay all within this range. From a mathematical point of view a longer constant period means a restriction of degrees of freedom. Therefore, the erythrocytes

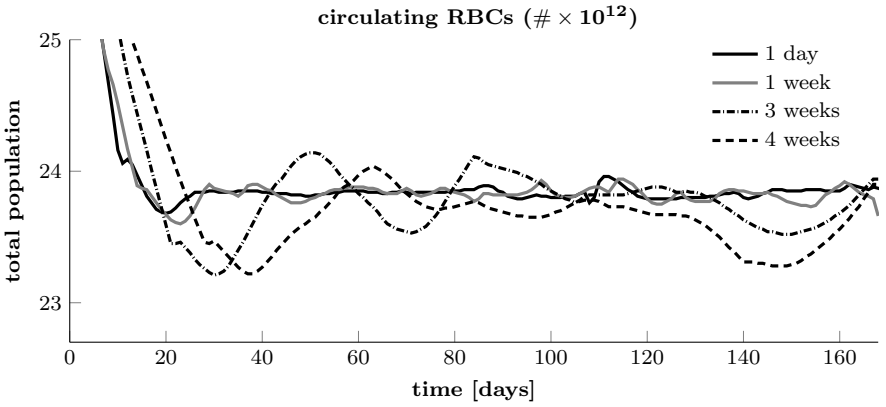

Fig. 11 Patient 4: optimal total RBC population for different constant periods. The visible range is the lower half of the target range.

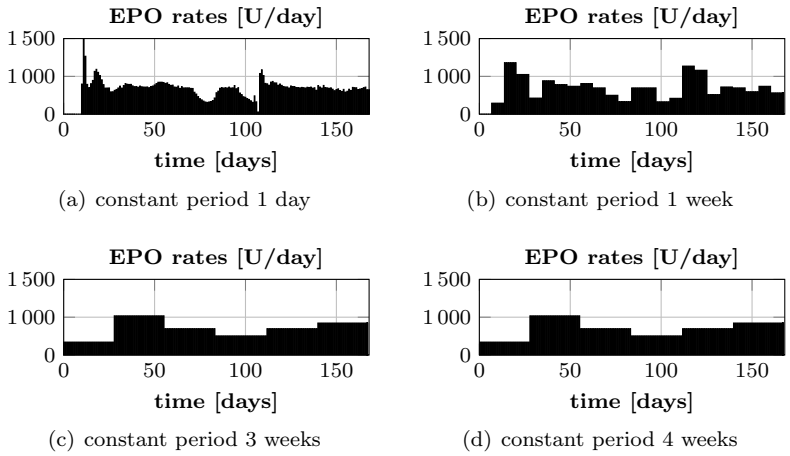

(a) constant period 1 day

(b) constant period 1 week

(c) constant period 3 weeks

(d) constant period 4 weeks

Fig. 12 Patient 4: optimal EPO rates for different constant periods.

population is best controllable for the shortest constant period. This is why the total RBC population is closest to the target where the controller can adjust the doses on a daily basis. And the longer the constant period is the larger are the oscillations around this line. But still, considering the small window we have plotted in Figure 11, the total populations are all nicely within this desired range. The corresponding total EPO doses, see Table 3, differ only little since the control cost penalization is comparable and since also for longer constant periods the total erythrocytes population can be brought and kept near the target state with similar EPO rates.

Table 3 Patient 4: total EPO doses for different constant periods.

Constant period	1 day	1 week	3 weeks	4 weeks
total dose [U]	55 598	56 964	56 721	57 695

6 Conclusion

The presented NMPC algorithm shows excellent results on the tested patient models. Although their clinical characteristics differ considerably from each other we can even define one fixed optimization setting for achieving stable Hgb levels in all of them. Nevertheless, to minimize EPO doses the parameter for control costs penalization should be tuned individually. The NMPC method requires a relatively long horizon in order to account for the system's large time delay. Given a sufficient horizon length the controller handles this delay superbly as well as simulated bleedings, missed treatments and EPO dosing errors. For these events an increase of the maximum allowed administration rate can improve the result. We observe that the restriction of EPO administration rates to be constant over a number of weeks results in slight oscillations of the total RBC population around the target state. However, even for a constant period of four weeks the oscillations are very small.

Our NMPC framework allows to easily change the desired Hgb level. Hence, individualized Hgb targets could be set directly. Future research has to address two aspects: first, the control structure needs to be changed such that EPO is only administered during dialysis treatments (in general three times per week). Second, it must be figured out how to correct/update the model over time based on measurements. In summary, the presented NMPC algorithm has the potential to bring more patients in the Hgb target range while decreasing Hgb variability and EPO utilization.

A Parameters for the model and the methods

In Tables 4-8 we present all parameters and units utilized in our numerical experiments. The rate of apoptosis for patients 3 and 4 are given in Figure 13.

References

Barbieri C, Bolzoni E, Mari F, Cattinelli I, Bellocchio F, Martin JD, Amato C, Stopper A, Gatti E, Macdougall IC, Stuard S, Canaud B (2016) Performance of a predictive model for long-term hemoglobin response to darbepoetin and iron administration in a large cohort of hemodialysis patients. PLOS ONE 11:1–18

Bequette BW (2013) Algorithms for a closed-loop artificial pancreas: The case for model predictive control. J Diabetes Sci Technol 7(6):1632–1643

Bermudez A, Vazquez ME (1994) Upwind methods for hyperbolic conservation laws with source terms. Computers & Fluids 23(8):1049–1071

Berns JS, Elzein H, Lynn RI, Fishbane S, Meisels IS, Deoreo PB (2003) Hemoglobin variability in epoetin-treated hemodialysis patients. Kidney Int 64(4):1514–21

Table 4 Fixed model parameters, values and units.

Par.	Meaning	Value	Unit
β_1	Proliferation rate for BFU-E cells	0.6	1/day
β_2	Proliferation rate for CFU-E cells	1.2	1/day
β_3	Proliferation rate for erythroblasts	0.723	1/day
$\overline{x}_1$	Maximal maturity for BFU-E cells	3	Days
$\underline{x}_2$	Minimal maturity for CFU-E cells	3	Days
$\overline{x}_2$	Maximal maturity for CFU-E cells	8	Days
$\underline{x}_3$	Minimal maturity for erythroblasts	8	Days
$\overline{x}_3$	Maximal maturity for erythroblasts	13	Days
$\underline{x}_4$	Minimal maturity for marrow reticulocytes	13	Days
$\overline{x}_4$	Maximal maturity for marrow reticulocytes	15.5	Days
α_4	Rate of ineffective erythropoiesis	0.09	1/day
α_5^0	Intrinsic mortality rate for erythrocytes	0.002	1/day
$\widehat{\Omega}_5$	Age interval for erythrocytes, where neocytolysis is possible	[14,34]	Days
ε	Regularization parameter for the mortality rate	10^{-8}	–
τ_E	EPO threshold for neocytolysis	80	mU/ml

Table 5 Fixed μ-parameters, values and units.

Parameter	Meaning	Value	Unit
μ_1	Constant for the sigmoid apoptosis rate for CFU-E cells	0.5	1/day
μ_3	Constant for the sigmoid apoptosis rate for CFU-E cells	0.5	Dimension-less
μ_4, μ_5	Constants for the sigmoid maturation velocity for marrow reticulocytes	2, 0.35	Dimension-less
μ_7	Constant for the sigmoid maturation velocity for marrow reticulocytes	2.3	Dimension-less
μ_8	Constant in the mortality rate for erythrocytes	$3.5 \cdot 10^3$	$\mathrm{mU}^3/\mathrm{ml}^2$
μ_9	Constant in the mortality rate for erythrocytes	3	$\mathrm{mU}^3/\mathrm{ml}^2$
μ_{10}	Constant in the mortality rate for erythrocytes	0.1	$\mathrm{mU}^3/\mathrm{ml}^2$

Table 6 Individualized model parameters and units.

Parameter	Meaning	Unit
c_{tbv}	Total blood volume	ml
$\overline{x}_5$	Maximal life span for erythrocytes	Days
S_0	Rate at which cells are committing to the erythroid lineage	1/day
E^{end}	Assumed constant endogenous EPO concentration in plasma	mU/ml
$T_{1/2}$	Half-life of Epoetin-α	1/day

Table 7 Individualized μ-parameters and units.

Parameter	Meaning	Unit
μ_2	Constant for the sigmoid apoptosis rate for CFU-E cells	ml/mU
μ_6	Constant for the sigmoid maturation velocity for marrow reticulocytes	ml/mU

Table 8 Individualized parameters for considered patients.

Parameter	Patient No. 1	2	3	4	5
c_{tbv}	3567	7373	4543	6102	2600
E^{end}	42.60	79.42	282.46	43	79
μ_2	0.016	0.009	0.008	0.011	0.010
μ_6	0.122	0.049	0.072	0.049	0.032
$T_{1/2}$	4.78	9.65	5.59	10.80	5.12
$\overline{x}_5$	92.3	74.3	43.1	94.8	50.5

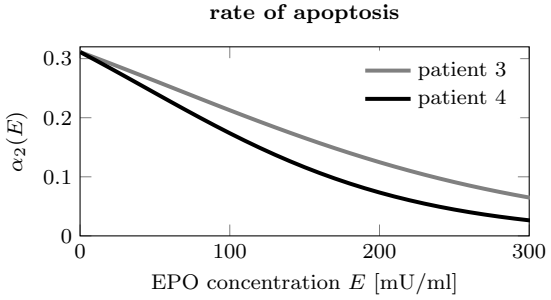

Fig. 13 Sigmoid function α_2 for patients 3 and 4.

Brier ME, Gaweda AE (2011) Predictive modeling for improved anemia management in dialysis patients. Curr Opin Nephrol Hypertens 20(6):573–6

Brier ME, Gaweda AE, Dailey A, Aronoff GR, Jacobs AA (2010) Randomized trial of model predictive control for improved anemia management. Clin J Am Soc Nephrol 5(5):814–20

DOPPS (2017) Arbor research collaborative for health: DOPPS practice monitor. URL http://www.dopps.org/DPM/ (accessed 29 Nov 2017)

Fishbane S, Berns JS (2005) Hemoglobin cycling in hemodialysis patients treated with recombinant human erythropoietin. Kidney Int 68(3):1337–43

Fishbane S, Berns JS (2007) Evidence and implications of haemoglobin cycling in anaemia management. Nephrol Dial Transplant 22(8):2129–32

Fuertinger DH (2012) A model of erythropoiesis. PhD thesis, Karl-Franzens University Graz

Fuertinger DH, Kappel F, Thijssen S, Levin NW, Kotanko P (2013) A model of erythropoiesis in adults with sufficient iron availability. J Math Biol 66(6):1209–1240

Grüne L, Pannek J (2011) Nonlinear Model Predictive Control. Communications and Control Engineering. Springer, London

Ito K, Kappel F (2002) Evolution equations and approximations. World Scientific, Singapore

Kappel F, Zhang K (1993) Approximation of linear age-structured population model using legendre polynomials. J Math Anal Appl 180:518–549

KDIGO (2012) Clinical practice guideline for anemia in chronic kidney disease. Kidney Int Suppl 2:279–335

Kelley CT (1999) Iterative Methods for Optimization. Frontiers in Applied Mathematics, SIAM, Philadelphia, PA

LeVeque RJ (1992) Numerical methods for conservation laws, 2nd edn. Lectures in Mathematics ETH Zürich, Birkhäuser, Berlin

Ma J, Dou Y, Zhang H, Thijssen S, Williams S, Kuntsevich V, Ouellet G, Wong MMY, Persic V, Kruse A, Rosales L, Wang Y, Levin NW, Kotanko P (2017) Correlation between inflammatory biomarkers and red blood cell life span in chronic hemodialysis patients. Blood Purif 43:200–205

Mactier R, Davies S, Dudley C, Harden P, Jones C, Kanagasundaram S, Lewington A, Richardson D, Taal M, Andrews P, Baker R, Breen C, Duncan N, Farrington K, Fluck R, Geddes C, Goldsmith D, Hoenich N, Holt S, Jardine A, Jenkins S, Kumwenda M, Lindley E, McGregor M, Mikhail A, Sharples E, Shrestha B, Shrivastava R, Stedden S, Warwick G, Wilkie M, Woodrow G, Wright M (2011) Summary of the 5th edition of the renal association clinical practice guidelines (2009-2012). Nephron Clin Pract 118(Suppl 1):27 – 70

Magni L, Raimondo DM, Bossi L, Man CD, De Nicolao G, Kovatchev B, Cobelli C (2007) Model predictive control of type 1 diabetes: an in silico trial. J Diabetes Sci Technol 1(6):804–12

Pottgiesser T, Specker W, Umhau M, Dickhuth HH, Roecker K, Schumacher YO (2008) Recovery of hemoglobin mass after blood donation, vol 48. Transfusion

Quarteroni A (2009) Numerical models for differential problems. MS&A. Springer, Milano

Rawlings JB, Mayne DQ (2009) Model Predictive Control: Theory and Design. Nob Hill Pub.

Strikwerda JC (2004) Finite Difference Schemes and Partial Differential Equations. Springer, Philadelphia

Strippoli GF, Craig JC, Manno C, Schena FP (2004) Hemoglobin targets for the anemia of chronic kidney disease: a meta-analysis of randomized, controlled trials. J Am Soc Nephrol 15:3154–65

Trangenstein JA (2009) Numerical solution of hyperbolic partial differential equations. Cambridge University Press, New York

Yang W, Israni RK, Brunelli SM, Joffe MM, Fishbane S, Feldman HI (2007) Hemoglobin variability and mortality in esrd. J Am Soc Nephrol 18(12):3164–70